IN-34
17066
12P

NASA Technical Memorandum 106646

Coupled Marangoni-Benard/Rayleigh-Benard Instability With Temperature Dependent Viscosity

J. Raymond Lee Skarda
Lewis Research Center
Cleveland, Ohio

and

Frances E. McCaughan
Case Western Reserve University
Cleveland, Ohio

Prepared for the
Winter Annual Meeting
sponsored by the American Society of Mechanical Engineers
Chicago, Illinois, November 6–11, 1994

(NASA-TM-106646) COUPLED MARANGONI-BENARD/RAYLEIGH-BENARD INSTABILITY WITH TEMPERATURE DEPENDENT VISCOSITY (NASA. Lewis Research Center) 12 p

N94-37507

Unclas

G3/34 0017066

National Aeronautics and
Space Administration

COUPLED MARANGONI-BENARD/RAYLEIGH-BENARD INSTABILITY WITH TEMPERATURE DEPENDENT VISCOSITY

J. Raymond Lee Skarda
National Aeronautics and Space Administration
Lewis Research Center
Cleveland, Ohio 44135

and

Frances E. McCaughan
Case Western Reserve University
Cleveland, Ohio 44106

ABSTRACT

The onset of convection induced by coupled surface tension gradient and buoyancy forces is investigated with temperature dependent viscosity. Both surface tension and viscosity are assumed to vary linearly with temperature. The linear viscosity approximation was found to be an adequate representation of relevant published experimental data. One limiting case, Ma = 0, is the buoyancy driven convection problem typically referred to as the Rayleigh-Benard stability problem. The other limiting case, Ra = 0, is the surface tension (gradient) driven flow problem referred to as the Marangoni-Benard problem. Several investigations of the Rayleigh-Benard problem with temperature dependent viscosity have been reported. One stability investigation of the Marangoni-Benard problem with a linear viscosity variation has also been published. Results from that Marangoni-Benard study indicate that linear viscosity variation is destabilizing while similar studies for the variable-viscosity-Rayleigh-Benard problem suggest that the above viscosity profile is stabilizing. In this study the variable viscosity analysis is extended to the coupled problem, which bridges the above limiting cases.

The equations and boundary conditions obtained from the linear analysis are solved numerically as a generalized eigenvalue problem. Neutral stability curves for different viscosity slopes are generated for the Marangoni-Benard and Rayleigh-Benard problems. It is shown that the curves can be collapsed to a single curve by appropriately scaling the results for each of the limiting cases. The critical Marangoni number is determined as a function of the slope of the viscosity temperature variation, ε, for different values of the Rayleigh number. Regression analyses of the numerical results are performed to provide a convenient means of computing the critical Marangoni number as a function of ε and the Rayleigh number. The linear temperature-dependent viscosity considered in this analysis gives results which are consistent with the Rayleigh-Benard studies employing an exponentially temperature-dependent viscosity. When the viscosity decreases linearly with temperature, the coupled buoyancy-surface tension problem, including the limiting special cases of Ra = 0 and Ma = 0, is found to be more stable than the constant viscosity case. The difference between this and the previous Marangoni-Benard study is explained.

NOMENCLATURE

a-f	finite difference coefficients (Eqs. (21) and (22))
Bi_s	surface Biot number
c_1,c_2	proportionality constants for ΔT_c
d	fluid layer thickness or depth
g	gravitational acceleration (or finite diff. coef for Eqs. (21) and (22)
h	surface heat flux temperature gradient
i	$\sqrt{-1}$
k	thermal conductivity
$\hat{k}$	unit vector in z direction
Ma	Marangoni number
P	pressure
p	pressure disturbance
Pr	Prandtl number
Q	surface heat flux
Ra	Rayleigh number
T	temperature
t	time
ΔT	temperature difference
$\bar{U}$	velocity vector
w	velocity disturbance amplitude
$\bar{u}$	velocity disturbance vector
x,y,z	cartesian coordinates

Greek symbols

α	wavenumber
β	base temperature gradient
ε	viscosity - temperature slope
κ	thermal diffusivity
λ	eigenvalue (dimensionless frequency)
μ	dynamic viscosity
ν	kinematic viscosity
θ	temperature disturbance
ϕ	temperature disturbance amplitude

ρ	fluid density
σ	surface tension
ξ	volumetric thermal expansion coefficient

Subscripts

0	parameter/variable value at lower surface
b	base quantity
CL	result based on Cloot and Lebon '85
c	critical value
d	parameter/variable value across fluid layer
max	maximum value
min	minimum value
s	property/parameter value at upper surface

Superscripts

mb	Marangoni-Benard (Ra=0)
rb	Rayleigh-Benard (Ma=0)
T	Transpose (see eqs. 2 and 11)
*	dimensional quantity

INTRODUCTION

The onset of cellular convection with temperature gradients imposed normal to the free surface continues to be an active research topic as illustrated by Koschmeider's (1993) extensive literature survey. Microgravity science applications of thermocapillary flows have motivated the study of surface tension induced instability known as the Marangoni-Benard problem in both one-g and microgravity environments (Legros, J.C., et al. 1990). In space, the effect of buoyancy is minimal and one can consider surface tension to be the sole driving force. Then the temperature difference necessary to achieve the critical Marangoni number, Ma_c, depends only on the fluid properties and fluid thickness. On the other hand, in ground-based studies of surface tension driven problem, Ma_c is also influenced by buoyancy, that is by the Rayleigh number. To minimize the effect of buoyancy in the one-g environment, the liquid layer must be thin but this means that a larger temperature difference must be imposed across the layer of fluid in order to reach the critical Marangoni number. As the temperature difference increases it is no longer appropriate to use constant values for the fluid properties. The effect of variable fluid properties on Ma_c becomes an important consideration.

The strong dependence of viscosity on temperature for most fluids, has prompted several studies of the onset of cellular convection which include this feature, (Palm, 1960, Stengel et. al.,1982, White, 1988, and Koschmeider, 1993). The studies almost exclusively consider the buoyancy induced instability problem. In fact, only one study treats the surface tension driven instability with a temperature dependent viscosity (Cloot and Lebon, 1985). For small to moderate viscosity variations, Stengel et al. and White found that the variable viscosity had a stabilizing effect on the Rayleigh-Benard problem while Cloot and Lebon concluded that the viscosity variation is destabilizing for the Marangoni-Benard problem. In this paper we investigate the effects of variable viscosity on the combined buoyancy and surface tension driven instability which was originally considered by Nield (1964). The Marangoni-Benard and Rayleigh-Benard instabilities are discussed as special cases. Viscosity is assumed to depend linearly on temperature throughout the study.

The governing equations and boundary conditions are developed in the following section. The numerical solution of the resulting eigenvalue problem is briefly discussed. The neutral stability curves for several viscosity-temperature slopes are presented and these show the stabilizing effect of variable viscosity for both the Marangoni-Benard and Rayleigh-Benard instabilities (for small viscosity variations). After rescaling the neutral stability results with the limiting critical parameter values, the variable viscosity curves are shown to collapse onto the constant viscosity curve. Variable viscosity results for the coupled surface tension and buoyancy induced instability are then compared with Nield's constant viscosity results. The relative contribution of the surface tension and buoyancy in establishing the instability is shown as a function of fluid depth for a high Prandtl number fluid, silicone oil, and a low Prandtl number fluid, mercury. The critical temperature difference across the fluid layer indicating that the fluid has lost linear stability, ΔT_c, and the corresponding viscosity-temperature slope, ε, are shown as functions of the fluid depth for both fluids. The validity of the linear viscosity profile which depends on ΔT_c is then examined as a function of the layer thickness, d.

DEVELOPMENT OF EQUATIONS

A temperature difference is imposed normal to the free surface of a thin liquid layer of fluid of infinite horizontal extent and finite thickness, d, as shown in Figure 1. The initial steady state or base state of the system is one of no fluid motion, with a linear temperature profile across the layer. The velocity and temperature profiles illustrated in Fig. 1 can immediately be expressed as, $U_b^* = 0$ and $T_b^* = T_{b0}^* - \beta z^*$. Using the notation of Pearson (1958) and Chandrasehkar (1981), U_b^* and T_b^* are respectively, the base flow velocity and temperature where the asterisk "*" denotes dimensional quantities and the subscript "b" denotes that this solution is the base flow. The temperature gradient of the base state, β is defined as $\beta = -dT_b^*/dz^*$ or $\beta = \Delta T_d^*/d$ where $\Delta T_d^* = T_{b0}^* - T_{bs}^*$. The lower surface is rigid and is held at a constant temperature. The upper surface is free and exchanges heat with the environment . It is well known that the deformation of the free surface also affects the critical temperature difference which leads to fluid motion, but in this study we focus on the variable viscosity effect and assume that the free surface is flat. First we give the nondimensional form of the governing equations and in the next section we linearize about the base state just described in order to determine whether small disturbances to the base state will grow or decay.

Specifically we are interested in the critical values of the nondimensional parameters where the change of stability occurs.

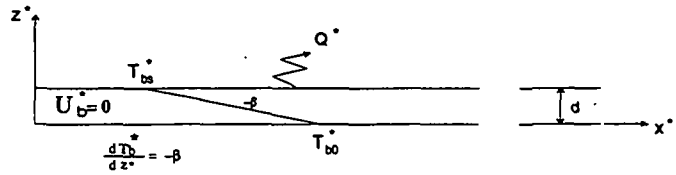

Figure 1. Base State For Thin Liquid Layer Of Infinite Extent

Nondimensional forms of mass, momentum, and energy equations for an incompressible fluid with the Boussinesq approximation are given in Eqs. (1) to (3). The derivation of these equations with the Boussinesq approximation and constant viscosity and their subsequent nondimensionalization are well known and we refer the interested reader to Chandrasekar (1981), and Drazin & Reid (1982) for details. Since dynamic viscosity is the fluid property which depends most strongly on temperature, in our study we permit the dynamic viscosity to vary with temperature while all other thermophysical properties apart from density and surface tension, are assumed constant. The inclusion of variable viscosity into the governing equations is discussed by Stengel et. al. (1982).

$$\bar{\nabla}\cdot\bar{U}=0 \tag{1}$$

$$\frac{D\bar{U}}{Dt}=-\bar{\nabla}P+\hat{k}\cdot RaPr(T-T_{b0})+ Pr\bar{\nabla}\cdot\left(\mu(T)\left[\bar{\nabla}\bar{U}+\left(\bar{\nabla}\bar{U}\right)^T\right]\right) \tag{2}$$

$$\frac{DT}{Dt}=\bar{\nabla}^2T \tag{3}$$

$\bar{U}$, T, P, t are the velocity vector, temperature, pressure, and time respectively. The reference values used to nondimensionalize the variables; length, velocity, temperature, pressure, and time are d, κ_0^*/d, βd, $\rho_0^*\kappa_0^*/d^2$, d^2/κ_0^*, respectively. ρ_0^* is the fluid density and κ_0^* is the fluid thermal diffusivity. The subscript 0 indicates that the properties are chosen at the lower surface temperature, T_{b0}. The characteristic value of the dynamic viscosity of the fluid, μ, is denoted as μ_0^*. These reference values are consistent with those used in the buoyancy instability studies presented in Chandrasekhar (1981) and Drazin and Reid (1982), and the surface tension instability investigations of Pearson (1958) and Scriven and Sternling (1964). Two dimensionless groups appear in the momentum equation, the Prandtl number, Pr, and the Rayleigh number, Ra, which are defined as follows:

$$Pr=\frac{\mu_0^*}{\rho_0^*\kappa_0^*} \qquad Ra=\frac{\rho_0^*\beta d^4\xi_0^* g}{\kappa_0^*\mu_0^*}$$

ξ_0^* is the volumetric thermal expansion coefficient and g is gravitational acceleration in the negative z-direction. The dot product of the unit vector in the z direction, $\hat{k}$, and the buoyancy (RaPr) term in Eq. (2) indicates that buoyancy only acts in the vertical direction. Therefore the Rayleigh number occurs only in the z-momentum equation.

The relationship showing how viscosity depends on temperature, $\mu(T)$, is given by Eq. (4). This equation is a first order expansion of $\mu(T)$ expanded about T_{b0} where $\varepsilon=\left.\frac{\partial\mu}{\partial T}\right|_{T_{b0}}$. Substituting Eq. (4) into the momentum equation, and expanding the viscous terms in the momentum equation leads to equation (5).

$$\mu(T)=1+\varepsilon(T-T_{b0}) \tag{4}$$

$$\frac{D\bar{U}}{Dt}=-\bar{\nabla}P+\hat{k}\cdot RaPr(T-T_{b0})-Pr\varepsilon\left[\bar{\nabla}T\cdot\bar{\nabla}\bar{U}+\bar{\nabla}T\cdot\left(\bar{\nabla}\bar{U}\right)^T\right]+ Pr\left(1+\varepsilon(T-T_{b0})\right)\bar{\nabla}^2\bar{U} \tag{5}$$

When ε = 0, Eq. (5) reduces to the constant viscosity momentum equation. The effect of the parameter, ε, on the stability of the quiescent base state is the primary focus of this paper.

The nondimensional boundary conditions are given by Eqs. (6) and (7). Equations (6(a) to (c)) represent the no-slip conditions and impenetrable wall condition at z = 0. Equation (6(d)) is the constant temperature condition along the wall. The normal stress boundary condition reduces to (Eq. 7(a)) when the free surface at z = 1 is assumed to be flat. Boundary condition (Eq. 7(b)) is the heat flux balance at the free surface, where Q* is the dimensional surface heat flux to the environment and k_0^* is the fluid thermal conductivity. Equation 7(c) is the vector equation for the tangential force balance along the free surface and it can be resolved into two equations in the x and y directions.

at $z=0$; $\bar{U}(0)=(U_x,U_y,U_z)=0$; $T(0)=T_{b0}$ (6(a) to (d))

at $z=1$; $U_z(1)=0$; $\frac{\partial T}{\partial z}+\frac{Q^*}{k_0^*b}=0$, (7(a),(b))

$$-\mu(T)\left[\left(\frac{\partial U_z}{\partial x}+\frac{\partial U_x}{\partial z}\right)\hat{i}+\left(\frac{\partial U_z}{\partial y}+\frac{\partial U_y}{\partial z}\right)\hat{j}\right]= Ma\nabla_{II}T \tag{7(c)}$$

The operator, ∇_{II}, is the surface gradient defined as $\hat{i}\frac{\partial}{\partial x}+\hat{j}\frac{\partial}{\partial y}$ where, $\hat{i}$ and $\hat{j}$ are unit vectors in the x and y directions respectively. The Marangoni number, Ma, which occurs in Eq. 7(c), is defined as: $Ma=\frac{\beta\, d^2\gamma_0^*}{\kappa_0^*\mu_0^*}$, where

parameter, γ_0^*, is defined as $\left.\frac{\partial \sigma^*}{\partial T^*}\right|_{T_{bs}}$, and is often referred to as the temperature variation of surface tension (Nield 1964 and Adamson 1967) or the differential coefficient of surface tension change with temperature (Scriven and Sternling 1964). The surface tension, σ^*, does not appear in our equations or boundary conditions since we have assumed a flat interface. Further discussion of the nondimensionalization of the free surface boundary conditions is found in Scriven and Sternling (1964), and Koschmeider (1993).

The surface heat flux, Q^*, has to be expressed in a form that is suitable for linearizing the heat flux boundary condition, Eq. (7). This is accomplished by expanding Q^* about the base state surface temperature, T_{bs}^*. The first order expansion is given by Eq. (8). As previously noted, the base state varies only in the z-direction. Therefore, $Q^*(T_{bs})$ can be re-expressed using Fourier's law by Eq. (9).

$$Q^*(T^*) = Q^*(T_{bs}^*) + \left.\frac{\partial Q^*}{\partial T^*}\right|_{T_{bs}^*} (T^* - T_{bs}^*) \tag{8}$$

$$Q^*(T_{bs}^*) = -k_0^* \left.\frac{dT^*}{dz^*}\right|_{z^*=d} = k_0^* \beta \tag{9}$$

Substituting Eq. (8) into Eq. (7(b)), using $k_0^*\beta$ in place of $Q^*(T_{bs}^*)$ and defining $h^* = \left.\frac{\partial Q^*}{\partial T^*}\right|_{T_{bs}^*}$, the dimensionless heat flux boundary condition becomes:

$$\frac{\partial T}{\partial z} + 1 + Bi_s(T_s - T_{bs}) = 0 \tag{10}$$

The dimensionless group, Bi_s, is defined as $Bi_s = \frac{h^* d}{k_0^*}$ and is referred to as either the surface Biot number (Pearson, 1958 and Nield, 1964) or the surface Nusselt number (Scriven and Sternling, 1964).

We note that the three-dimensional mass, momentum, and energy equations are given in Eqs. (1) to (3), yet the boundary conditions are only specified in the z-direction. After the governing equations and boundary conditions are linearized and simplified using some vector operations, it is clear that the x and y components do not affect the stability of the base state. Equations ((1), (3), (5), and (6)), and Eqs. (7(a) and (10)) make up the system which we will linearize in the next section.

Linearize Governing Equations

The dependent variables are written in terms of the following base flow and perturbation variables:

$$\bar{U} = \bar{u}, \qquad T = T_b + \theta, \qquad \Delta P = \Delta P_b + \Delta p$$

After substituting for T_b and $\bar{\nabla} T_b$, the disturbance equations for temperature dependent viscosity become:

$$\frac{\partial \bar{u}}{\partial t} = -\bar{\nabla} p + \hat{k} \cdot Ra Pr \theta - Pr \varepsilon \left[\hat{k} \cdot \left(\bar{\nabla} \bar{u} + (\bar{\nabla} \bar{u})^T \right) \right] + Pr(1 - \varepsilon z) \bar{\nabla}^2 \bar{u} \tag{11}$$

$$\frac{\partial \theta}{\partial t} - u_z = \bar{\nabla}^2 \theta \tag{12}$$

$\hat{k}$ is the unit vector in the z-direction shown in Fig. 1. The curl operator is applied twice to the momentum equation, Eq. (11), which yields Eq. (13).

$$\frac{\partial (\nabla^2 \bar{u})}{\partial t} = \hat{k} \cdot \left(Ra\, Pr\, \bar{\nabla}_{//}^2 \theta - 2 Pr\, \varepsilon \frac{\partial (\nabla^2 \bar{u})}{\partial z} \right) + Pr(1 - \varepsilon z) \nabla^4 \bar{u} \tag{13}$$

The first curl operation yields the vorticity equation and eliminates the pressure terms. The second curl operation decouples the x and y momentum equations from the z-momentum and the energy equations. The z-momentum and energy equations remain coupled through the buoyancy term in Eq. (13), the convective term in Eq. (12), and the tangential free surface boundary condition (discussed below). Furthermore, the relevant stability parameters, Ma and Ra, do not appear in either the x or y momentum equation or their associated boundary conditions. Given these considerations, Eq. (13) reduces to a scalar equation in u_z, Eq. (14).

$$\frac{\partial (\nabla^2 u_z)}{\partial t} = Ra\, Pr\, \nabla_{//}^2 \theta - 2 Pr\, \varepsilon \frac{\partial (\nabla^2 u_z)}{\partial z} + Pr(1 - \varepsilon z) \nabla^4 u_z \tag{14}$$

The boundary conditions for the perturbed variables associated with Eqs. (12) and (14) are given by Eqs. (15) and (16).

$$\text{at } z = 0,\ u_z = 0; \quad \frac{\partial u_z}{\partial z} = 0; \qquad \theta = 0 \qquad \text{(15(a) to (c))}$$

$$\text{at } z = 1,\ u_z = 0;\quad \frac{\partial\theta}{\partial z} + Bi_s\theta(1) = 0 \qquad \text{(16(a) and (b))}$$

$$-(1-\varepsilon)\left(\nabla^2_{//}u_z - \frac{\partial^2 u_z}{\partial z^2}\right) = Ma\nabla^2_{//}\theta \qquad \text{(16(c))}$$

Small Disturbance Analysis

Since Eqs. (12) and (14) are linear, we assume solutions for u_z and ϕ are of the form:

$$u_z = w(z)e^{i(\alpha_x x + \alpha_y y) + \lambda t} \quad \text{and} \quad \theta = \phi(z)e^{i(\alpha_x x + \alpha_y y) + \lambda t}$$

α_x and α_y are the dimensionless wavenumbers in the x and y directions, and λ is the dimensionless frequency. Substituting these into Eqs. (12) and (14) results in the following ordinary differential equations.

$$\lambda\phi(z) - D^2\phi(z) + \alpha^2\phi(z) - w(z) = 0 \qquad (17)$$

$$\lambda\left(D^2 w - \alpha^2 w(z)\right) = -Ra Pr\alpha^2\phi - 2\,Pr\,\varepsilon \times\left(D^3 w - \alpha^2 Dw\right) + Pr(1-\varepsilon z)\left(D^4 w - 2\alpha^2 D^2 w + \alpha^4 w(z)\right) \qquad (18)$$

where $D = \frac{d}{dz}$ and $\alpha^2 = \alpha_x^2 + \alpha_y^2$.

The boundary conditions at $z = 0$ reduce to:

$$w(0)=0, \quad Dw(0)=0, \quad \phi(0)=0. \qquad \text{(19(a) to (c))}$$

At $z = 1$, the flat interface condition, heat flux condition, and tangential stress boundary condition are:

$$w(1) = 0, \quad D\phi(1) + Bi_s\phi(1) = 0, \qquad \text{(20(a),(b))}$$

$$(1-\varepsilon)D^2 w = -\alpha^2 Ma\,\phi(1) \qquad \text{(20 (c))}$$

Equations (17) to (20) are solved to determine whether the velocity and temperature disturbances grow or decay for given values of the relevant parameters, Ma, Ra, ε, and α. This problem is also referred to as a temporally developing flow problem since the disturbance growth or decay is in time. For temporally developing flows, α_x and α_y are real and the eigenvalue, λ, is complex. If the real part of λ is positive the disturbance grows; if the real part of λ is negative the disturbance decays in time; and if λ is zero, the disturbance persists unchanged in time. Analytically determined approximate solutions may exist, such as the series solutions of Cloot and Lebon (1985) and Nield (1964), but we chose a finite difference approach because of its ease of implementation.

Equations (17) to (20) were discretized using a central difference scheme. The discretized governing equations, Eqs. (21) and (22), were arranged in the form $Az = \lambda Bz$, which is the generalized eigenvalue problem. In this analysis, coefficients, a through e are functions of z while f, g, and r are constants.

$$a(z_i)w_{i-2} + b(z_i)w_{i-1} + c(z_i)w_i + d(z_i)w_{i+1} + e(z_i)w_{i+2} + r\phi_i = \lambda\left(f w_{i-1} + g w_i + f w_{i+1}\right) \qquad (21)$$

$$f\phi_{i-1} + g\phi_i + f\phi_{i+1} + w_i = \lambda\left(\phi_i\right) \qquad (22)$$

B is a nonsingular matrix, so it is possible to reduce the system to a regular eigenvalue problem of the form $Cz = B^{-1}A = \lambda z$. Assuming a flat interface ensures that B is a tridiagonal matrix which can efficiently be inverted using a tridiagonal solver. For this investigation, the resolution was 50 points across the fluid layer in the z-direction. Since there are two differential equations the matrix problem has order 100. The nature of the boundary conditions permits this to be reduced to 99.

RESULTS

Neutral Stability Curves

The effects of variable viscosity on the neutral stability curves for the limiting cases, Marangoni-Benard and Rayleigh-Benard problems are shown in Figs. 2 and 3, respectively. Results are presented for an insulated free surface, $Bi_s = 0$, since this choice of Bi_s yielded the smallest values of Ma_c and Ra_c. With the above heat flux restriction the boundary conditions corresponding to the shown results are referred to as a rigid and conductive lower surface and a free and insulated upper surface. In both figures, the loci of points which give zero eigenvalues move upwards for increasingly negative values of viscosity slopes, ε's, clearly showing the stabilizing effect of the temperature-dependent viscosity. In Table 1 we have shown the percentage change of the critical Marangoni and Rayleigh numbers, relative to the case of constant viscosity. The temperature dependent viscosity has a slightly greater stabilizing effect on Ma_c^{mb} for the Marangoni-Benard problem, than on Ra_c^{rb} for the Rayleigh-Benard problem. The superscript "mb" emphasizes that this is the Marangoni-Benard problem, therefore the Rayleigh number is zero. The superscript "rb" denotes the Rayleigh-Benard problem therefore the Marangoni number is zero. This distinction will be important when the coupled buoyancy-surface tension problem is discussed.

It is also of interest to know the nature of the new flow which develops when the base flow loses stability. Some inkling of this can be obtained from the critical value of the wavenumber, α. In Figs. 2 and 3 the critical wavenumber appears unchanged by the variable viscosity, however Table 2 shows that the critical wavenumbers, α_c's, decrease slightly as ε becomes more negative.

The constant viscosity curve, $\varepsilon = 0$, was first given by Pearson for the case of a rigid and conductive lower surface

and a free and insulated upper surface. The simpler problem of constant viscosity permits a closed form solution of the eigenvalue problem and so formulae for the parameter values which give zero eigenvalues can be obtained. At smaller values of the wavenumber, α, our numerically computed Ma_c^{mb} agrees with Pearson's exact solution to three significant figures. But as the wavenumber is increased, the accuracy of the numerical results decreased. The maximum error in Ma_c^{mb} with respect to Pearson's results is 0.8% which occurs at $\alpha = 6$. We also compared our results with those of Nield for the Rayleigh-Benard problem. In that case, the critical Rayleigh number, Ra_c^{rb}, from the constant viscosity curve in Fig. 3 agreed with Nield's tabulated result within 0.1%.

The Marangoni-Benard problem with a linear temperature dependent viscosity profile and a deformable free surface was investigated previously by Cloot and Lebon (1985). They obtained an analytical solution for that problem in terms of a power series expansion. Cloot and Lebon concluded that a viscosity profile which decreases linearly with temperature, is destabilizing. Their conclusion contradicts the findings of the present analysis which shows the above viscosity profile to be stabilizing. We believe that this discrepancy occurred for the following reason. While Cloot and Lebon permitted the kinematic viscosity to vary in the momentum equation, they assumed a constant (dynamic) viscosity in the tangential and normal stress boundary conditions. Only the tangential boundary condition is important here since we assume that the interface is flat. The neutral stability results from Cloot and Lebon's, Ma_{CL}, are easily corrected for variable viscosity in the tangential boundary condition as follows: $Ma^{mb}(\varepsilon) = Ma_{CL} * (1-\varepsilon)$. After adjusting their solution in this manner we find that the results from their power series solution agree with the results presented above. Critical Marangoni numbers presented in Table 2 differ from the corrected Cloot and Lebon results by less than 0.1%.

Detailed investigations of the variable viscosity Rayleigh-Benard problem were performed by Stengel, Oliver, and Booker (1982) and White (1988). Stengel et al., considered rigid lower and free upper surfaces in addition to other surface conditions; however both surfaces were maintained at constant temperatures in all cases. White's configuration consisted of rigid and conductive (constant temperature) conditions on both surfaces. Since our boundary conditions are slightly different, the Rayleigh-Benard results shown in Fig. 3 can only be compared qualitatively with the Stengel et al. and White studies. Stengel et al. showed that when the viscosity decreases exponentially with temperature, corresponding to our $\varepsilon<0$, and when the ratio of ν_{max} (at T_{b0}^*), to ν_{min} (at T_s^*) is small to moderate, $\nu_{max}/\nu_{min} < 3000$, the effect is that the fluid is more stable. On the other hand they found that at larger viscosity variation ratios, the effect of the viscosity variation was to cause the fluid to go unstable at smaller values of critical Rayleigh number. White (1988) performed an extensiveset of experiments to study the onset of convection for the Rayleigh-Benard problem with temperature-dependent viscosity. He also observed that Ra_c^{rb} increases with an increase in viscosity variation for $\nu_{max}/\nu_{min} \leq O(1000)$. The results in Fig. 3 agree qualitatively with those of Stengel et al. and White. This agreement is expected since an exponential viscosity variation is well approximated by a linear variation for small ε. White also examined the effect of variable viscosity on the critical wavenumber and his numerical results show that the critical wavenumber decreases slightly with increasing viscosity variation for $\nu_{max}/\nu_{min} < 55$. This is consistent with the behavior of α_c observed in Table 2.

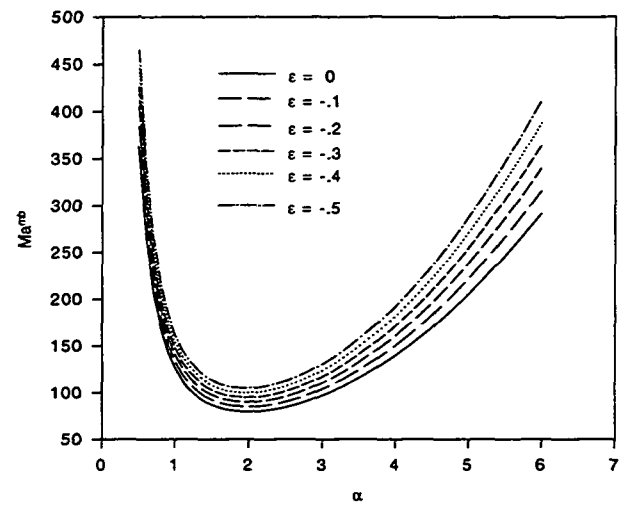

Figure 2 Marangoni-Benard Neutral Stability Curves For Different Viscosity-Temperature Slope Values, Ra=0

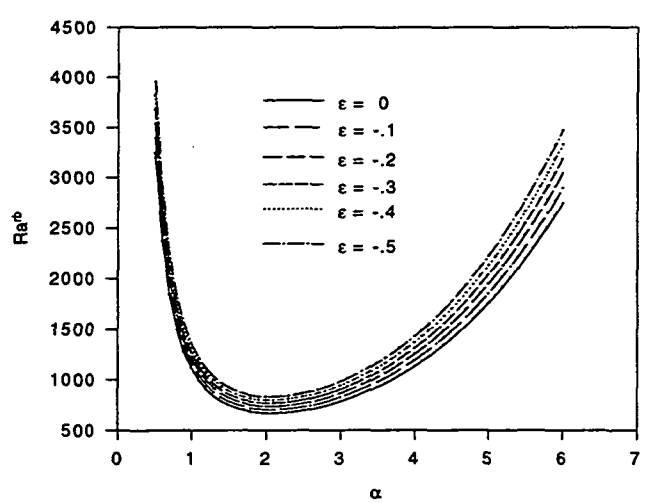

Figure 3. Rayleigh-Benard Neutral Stability Curves For Different Viscosity-Temperature Slope Values, Ma=0

Table 1.–Increase of Critical Marangoni Number and Critical Rayleigh Number For Marangoni-Benard and Rayleigh-Benard Problems

ε	$\frac{Ma_c(\varepsilon) - Ma_c(0)}{Ma_c(0)}$	$\frac{Ra_c(\varepsilon) - Ra_c(0)}{Ra_c(0)}$
0.	0.	0.
-.1	6.5	4.9
-.2	12.9	9.8
-.3	19.2	14.6
-.4	25.4	19.3
-.5	31.6	24.0

Table 2.–Critical Wavenumbers, Marangoni Numbers and Rayleigh Numbers For Different Viscosity Slopes

ε	$\alpha_c^{mb}(\varepsilon)$	$Ma^{mb}_c(\varepsilon)$	$\alpha_c^{rb}(\varepsilon)$	$Ra^{rb}_c(\varepsilon)$
0.0	1.991	79.6	2.085	668.3
-0.1	1.985	84.8	2.080	701.3
-0.2	1.974	89.9	2.075	733.8
-0.3	1.965	95.0	2.070	765.8
-0.4	1.958	99.9	2.066	797.3
-0.5	1.951	104.8	2.062	828.4

Scaling

In Fig. 4 we show that when the wavenumber is divided by its critical value, $\alpha_c(\varepsilon)$, and the Marangoni number is scaled by $Ma_c^{mb}(\varepsilon)$, the neutral stability curves for the Marangoni-Benard problem, collapse onto a single curve. This figure also includes the scaled results for the Rayleigh-Benard problem, where the wavenumber and Rayleigh number are divided by $\alpha_c(\varepsilon)$ and $Ra_c^{rb}(\varepsilon)$. This means that with a limited amount of information, $\alpha_c(\varepsilon)$ and $Ma_c^{mb}(\varepsilon)$, the neutral stability curve for a given viscosity slope, ε, can be approximated from Pearson's exact solution for the constant viscosity neutral stability curve. The same is true for the Rayleigh-Benard problem, where the neutral stability curve for $\varepsilon \neq 0$ can be obtained approximately by scaling the constant viscosity neutral stability curve with known values of $\alpha_c(\varepsilon)$ and $Ra_c^{rb}(\varepsilon)$. The maximum error that is incurred in this scaling process for the Marangoni and Rayleigh curves occurred for $\varepsilon = -0.5$ and is respectively 3% and 2%.

The dependence of the critical values of Marangoni and Rayleigh numbers and wavenumber on the slope of the viscosity temperature relation, ε, is shown in Fig. 5. This figure reveals that the critical Marangoni and critical Rayleigh numbers vary linearly with the viscosity slope, ε. For the range of ε considered, the α_c variation with ε can also be approximated as linear. The critical numbers, $Ma_c^{mb}(\varepsilon)$ and $Ra_c^{rb}(\varepsilon)$, are scaled by the constant viscosity critical numbers, $Ma_c^{mb}(0)$ and $Ra_c^{rb}(0)$. Linear regression results of the Figure 5 data are given by Eqs. (23) to (26). Values for $\alpha_c(\varepsilon)$, $Ma_c^{mb}(\varepsilon)$, $Ra_c^{rb}(\varepsilon)$ to three decimal places are given in Table 2.

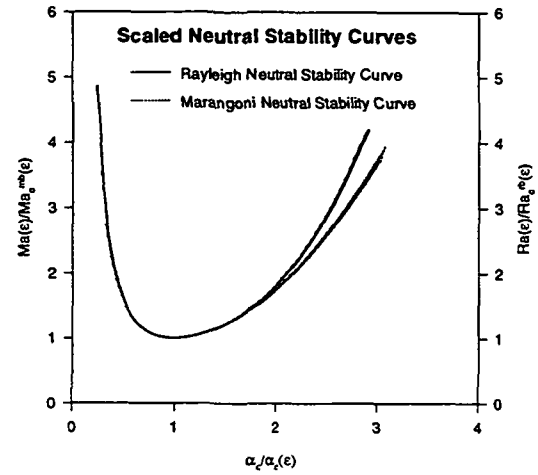

Figure 4. Scaled Rayleigh-Benard & Marangoni-Benard Neutral Stability Curves.

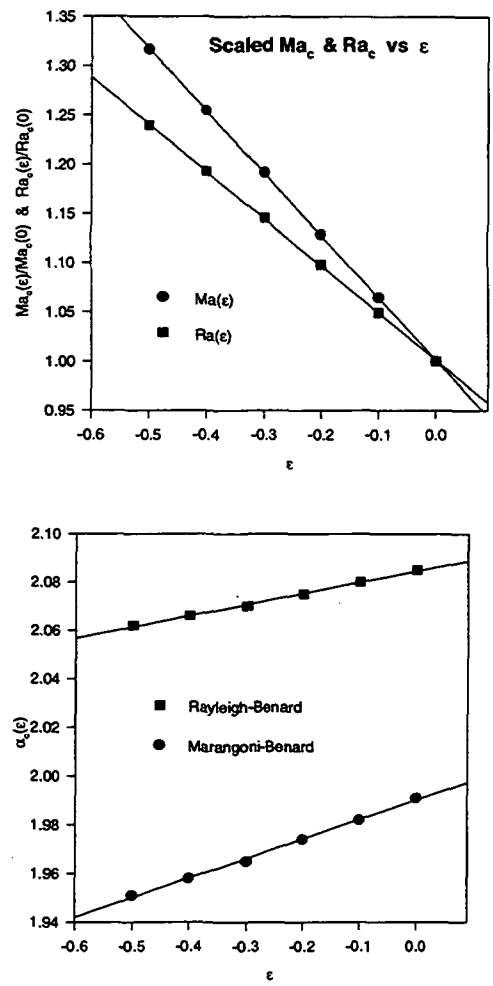

Figure 5. Critical Marangoni Number, Critical Rayleigh Number, and Critical Wavenumbers as a Function of Viscosity Temperature Slope

$$\frac{Ma_c^{mb}(\varepsilon)}{Ma_c^{mb}(0)} = 1.000 - .633\varepsilon \tag{23}$$

$$\frac{Ra_c^{rb}(\varepsilon)}{Ra_c^{rb}(0)} = 1.000 - .479\varepsilon \tag{24}$$

$$\alpha_c^{mb} = 1.990 + .080\varepsilon \tag{25}$$

$$\alpha_c^{rb} = 2.085 + .046\varepsilon \tag{26}$$

Coupled Buoyancy and Surface Tension Problem

The stability of a thin layer of fluid with a temperature gradient normal to the free surface with combined buoyancy and surface tension driving forces and constant viscosity was first solved by Nield. In that work it was shown that the buoyancy and surface tension forces "reinforced one another" with regard to the onset of convection. In other words, Ma_c and Ra_c are approximately inversely proportional for the constant viscosity coupled problem. Nield normalized the critical Marangoni Number, Ma_c, with the critical Marangoni number from the Marangoni-Benard problem, $Ma_c^{mb}(0)$. Similarly, the critical Rayleigh number, Ra_c was normalized with respect to the critical Rayleigh number from the Rayleigh-Benard problem, $Ra_c^{rb}(0)$. The interaction between the scaled critical values, Ma_c and Ra_c, for the coupled problem is shown in Fig. 6. In our case, we modified Nield's approach by scaling $Ma_c(\varepsilon)$ and $Ra_c(\varepsilon)$ by $Ma_c^{mb}(\varepsilon)$ and $Ra_c^{rb}(\varepsilon)$, respectively. The variable viscosity results shown in Fig. 6 are in excellent agreement with Nield's constant viscosity results. The greatest deviation from Nield's curve is $\approx 0.3\%$ and occurs for $\varepsilon = -0.5$ results. Equation (27) is a curve fit of the constant viscosity numerical data (Nield's curve) and is also shown in Fig. 6.

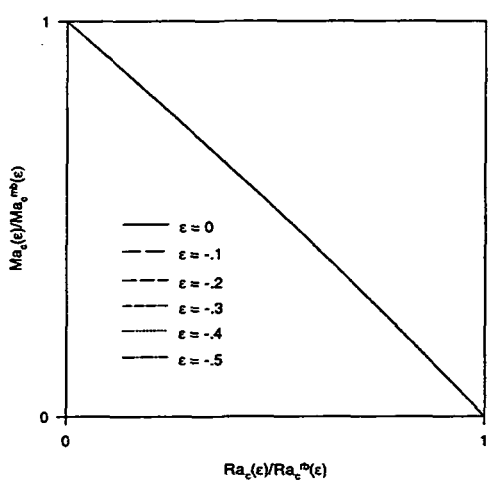

Figure 6 Scaled Critical Marangoni Numbers and Rayleigh Numbers For Different Viscosity Slope Variations

$$\frac{Ma_c(\varepsilon)}{Ma_c^{mb}(\varepsilon)} = 1 - \left(\frac{Ra_c(\varepsilon)}{Ra_c^{rb}(\varepsilon)}\right)^{1.055} \tag{27}$$

Equations (23) and (24) can be used to compute values of $Ma_c^{mb}(\varepsilon)$ and $Ra_c^{rb}(\varepsilon)$. Then using either Fig. 6 or Eq. (27), the critical values, $Ma_c(\varepsilon)$ and $Ra_c(\varepsilon)$ for the corresponding variable viscosity coupled problem can be determined.

The results from the previous section are used to investigate the stability of a thin layer for two different fluids, a large Prandtl number fluid, silicone oil, and a small Prandtl number fluid, mercury. Nield's curve, which is approximated by Eq. (27), is used to determine the "critical" temperature difference across the fluid layer, ΔT_c, and the dimensionless viscosity slope, ε, for varying fluid layer thicknesses, d. For a given fluid, the appropriate fluid layer thickness required for study of the surface tension dominated, buoyancy dominated, or coupled instability is also computed from Nield's curve. The critical temperature difference, ΔT_c, is computed by substituting Eqs. (23), (24), and the value of ε into Eq. (27) and iteratively solving the resulting relationship between, ΔT_c and d. After solving for ΔT_c, the curves in Figs. 7(a) and 8(a) were obtained by directly substituting ΔT_c, and d into the definitions of Ma_c/Ma_c^{mb} and Ra_c/Ra_c^{rb}. The critical temperature difference and the corresponding slope of viscosity versus temperature, ε, are plotted as functions of fluid depth, d, in Figs. 7(b) and 8(b).

Figures 7(a) and 8(a) provide a measure of the controlling instability mechanism, buoyancy or surface tension, at different fluid layer depths, d. The transition from a surface tension dominated instability to a buoyancy dominated instability, in 1 g, occurs at fluid depths of 7.5 mm for the silicone oil and 8.5 mm for mercury. We (arbitrarily) impose the limits $Ra_c/Ra_c^{rb} < .01$ to define the Marangoni-Benard instability and $Ma_c/Ma_c^{mb} < .01$ to define Rayleigh-Benard instability. In 1 g, the instability can be characterized as the Marangoni-Benard for fluid depths less than 1 mm for both silicone oil and mercury. For silicone oil and mercury depths greater than 7.25 cm and 8.15 cm, respectively, the Rayleigh-Benard instability occurs in a 1g environment. For 10^{-2}g, the Marangoni instability occurs for d less than 7.5 mm for silicone oil and 8 mm for mercury. At 10^{-4} g, the Marangoni-Benard instability persists beyond the 3.5 cm fluid depth shown in the figures.

Figures 7(b) and 8(b) show that the magnitude of both ΔT_c and the dimensionless viscosity slope, ε, decrease with increasing fluid depth, d. The ΔT_c curves for the reduced gravity case, 10^{-2} g, lie above the 1g curves in the above figures. The above observations are expected from the trends of the critical Marangoni and critical Rayleigh numbers as well as from an examination of Eq. (27). Approximating Nield's curve by truncating the 1.055 exponent in Eq. (27) to 1, and then solving for ΔT_c, we obtain the following approximate expression: $\Delta T_c \propto \frac{1}{c_1 d + c_2 g d^3}$. From this expression it is readily observed that ΔT_c decreases with an increasing fluid depth and gravity. The behavior of $-\varepsilon$ is identical to the ΔT_c behavior, with magnitude of ε scaled by μ_o and $d\mu^*/dT^*$.

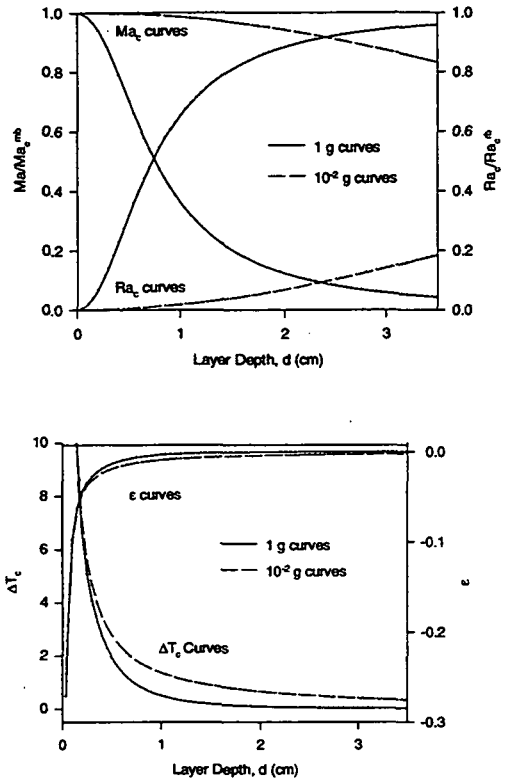

Figure 7. Critical Values for Different Fluid Depths for Silicone Oil

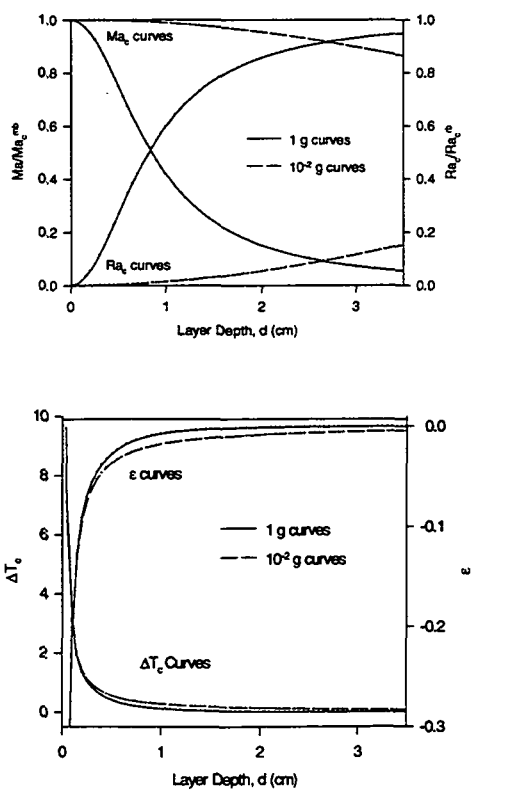

Figure 8 Critical Values for Different Fluid Depths for Mercury

Table 3 Thermal Physical Properties of Selected Fluids
Fluid Properties Taken At 300 K

Part (a)

Fluid	ε* kg/m^3	k* W/m-K	Cp* J/kg-K	μ* N-s/m^2
Silicone Oil[3]	968	.156	1507.2	.096800
Mercury[1,2]	13539	8.180	139.3	.001688

Part (b)

Fluid	ε* (dμ*/dT*) N-s/m^2-K	γ* (dσ*/dT*) N/m-K	ξ* 1/K
Silicone Oil[3]	-6.54e-4	-.00020	.00018
Mercury[1,2]	-5.35e-6	-.00006	.00096

The viscosity slopes, ε, shown in Figs. 7(b) and 8(b) suggest that the linear variable viscosity approximation is valid for $d \geq 1$ mm for silicone oil, and $d \geq 2$ mm for mercury. The variable viscosity effect is negligible, $\varepsilon \leq -.01$, for fluid depths greater than 9 mm for both the silicone oil and mercury.

CONCLUDING REMARKS

Viscosity which is permitted to vary linearly with temperature stabilizes the coupled Marangoni-Benard/ Rayleigh-Benard problem and both of the limiting cases, Rayleigh number equal to zero and Marangoni number equal to zero. A steeper (more negative) viscosity slope results in a greater stabilizing effect. Cloot and Lebon's conclusion that viscosity is destabilizing for the Marangoni-Benard problem needs to be adjusted to reflect the variable viscosity in the boundary conditions, by simply multiplying their critical Marangoni number results by (1-ε). The critical parameter values for the two limiting cases, Ma_c^{mb} and Ra_c^{rb}, were found to vary linearly with ε. Formulae showing the dependence of Ma_c^{mb} and Ra_c^{rb} behavior on the viscosity slope, ε, are given by Eqs. (23) and (24). These relations can be used to generate the variable viscosity neutral stability curves from the constant viscosity neutral stability curves for both the Marangoni-Benard and Rayleigh-Benard problems.

The variable viscosity (linear temperature dependence) results for the coupled Marangoni-Benard and Rayleigh-Benard problem collapse onto Nield's curve by appropriately scaling $Ra_c(\varepsilon)$ and $Ma_c(\varepsilon)$. The relative importance of buoyancy and surface tension to the Benard instability can be explicitly shown as a function of fluid layer depths. Specifying the fluid depth also fixes ΔT_c through Eq. (27). The parameter ε, is proportional to the temperature difference across the fluid layer, which equals ΔT_c at the bifurcation point. Since ΔT_c is a function of fluid depth, the validity of the small ε approximation at the bifurcation point that is, the critical parameter value where linear stability is lost, can be examined for different values of the fluid layer depth. It was determined that the linear variable viscosity approximation is valid for $d \geq 1$ mm for silicone oil, and $d \geq 2$ mm for mercury. When the

fluid depth exceeds 9 mm for both fluids, the bifurcation point can adequately be determined with a constant viscosity assumption.

REFERENCES

Adamson, A.W., Physical Chemistry of Surfaces, John Wiley & Son's, New York, 1967.

Chandrasekhar, S., Hydrodynamic and Hydromagnetic Stability, Dover, New York, 1981.

Cloot, A., and G. Lebon, "Marangoni Instability In a Fluid Layer With Variable Viscosity and Free Interface In Microgravity," PhysicoChemical Hydrodynamics, Vol. 6, 1985, pp. 453-462.

Incropera, F. P., and D. P. DeWitt, Fundamentals of Heat and Mass Transfer, John Wiley and Sons, New York, 1985.

Koschmieder, E.L., Benard Cells and Taylor Vorticies, Cambridge University Press, 1993.

Legros, J.C., O. Dupont, P. Queeckers, S. Van Vaerenbergh, and D. Schwabe, "Thermohydrodynamic Instabilities and Capillary Flow," Low Gravity Fluid Dynamics and Transport Phenomena, Ed J. Koster and R. Sani, American Institute of Aeronautics and Astronautics, 1990.

Nield, D. A., "Surface Tension and Buoyancy Effects In Cellular Convection," Journal of Fluid Mechanics, Vol. 19, 1964, pp. 341-352.

Ostrach, S., "Low-Gravity Fluid Flows," Annual Review of Fluid Mechanics, Vol. 14, 1982, pp. 313-345.

Pearson, J. R. A., "On Convection Cells Induced by Surface Tension," Journal Of Fluid Mechanics, Vol. 4, 1958, pp. 489-500.

Scanlon, J. W., and L. A. Segel, "Finite Amplitude Cellular Convection Induced By Surface Tension," Journal of Fluid Mechanics, Vol. 30, 1967, pp. 149-162.

Scriven, L. E., and C. V. Sternling, "On Cellular Convection Driven By Surface-Tension Gradients: Effects Of Mean Surface Tension and Surface Viscosity," Journal Of Fluid Mechanics, Vol. 19, 1964, pp. 321-340.

Smith, K. A., "On Convective Instability Induced By Surface Tension Gradients," Journal Of Fluid Mechanics, Vol. 24, 1966, pp. 401-414.

Stengel, K.C., D. S. Oliver, and, J. R. Booker, "Onset of Convection In a Variable-Viscosity Fluid," Journal of Fluid Mechanics, Vol. 120, 1982, pp. 411-431.

White, D.B., "The Planforms and Onset of Convection With a Temperature Dependent Viscosity," Journal of Fluid Mechanics, Vol. 191, 1988, pp 246-286.

REPORT DOCUMENTATION PAGE

Form Approved
OMB No. 0704-0188

Public reporting burden for this collection of information is estimated to average 1 hour per response, including the time for reviewing instructions, searching existing data sources, gathering and maintaining the data needed, and completing and reviewing the collection of information. Send comments regarding this burden estimate or any other aspect of this collection of information, including suggestions for reducing this burden, to Washington Headquarters Services, Directorate for Information Operations and Reports, 1215 Jefferson Davis Highway, Suite 1204, Arlington, VA 22202-4302, and to the Office of Management and Budget, Paperwork Reduction Project (0704-0188), Washington, DC 20503.

1. AGENCY USE ONLY (*Leave blank*)	2. REPORT DATE	3. REPORT TYPE AND DATES COVERED
	July 1994	Technical Memorandum

4. TITLE AND SUBTITLE

Coupled Marangoni-Benard/Rayleigh-Benard Instability With Temperature Dependent Viscosity

5. FUNDING NUMBERS

WU-674-24-05

6. AUTHOR(S)

J. Raymond Lee Skarda and Frances E. McCaughan

7. PERFORMING ORGANIZATION NAME(S) AND ADDRESS(ES)

National Aeronautics and Space Administration
Lewis Research Center
Cleveland, Ohio 44135-3191

8. PERFORMING ORGANIZATION REPORT NUMBER

E-8952

9. SPONSORING/MONITORING AGENCY NAME(S) AND ADDRESS(ES)

National Aeronautics and Space Administration
Washington, D.C. 20546-0001

10. SPONSORING/MONITORING AGENCY REPORT NUMBER

NASA TM-106646

11. SUPPLEMENTARY NOTES

Prepared for the Winter Annual Meeting sponsored by the American Society of Mechanical Engineers, Chicago, Illinois, November 6–11, 1994. J. Raymond Lee Skarda, NASA Lewis Research Center, and Frances E. McCaughan, Case Western Reserve University, Cleveland, Ohio 44106. Responsible person, J. Raymond Lee Skarda, organization code 6712, (216) 433-8728.

12a. DISTRIBUTION/AVAILABILITY STATEMENT

Unclassified - Unlimited
Subject Category 34

12b. DISTRIBUTION CODE

13. ABSTRACT ***(Maximum 200 words)***

The onset of convection induced by coupled surface tension gradient and buoyancy forces is investigated with temperature dependent viscosity. Both surface tension and viscosity are assumed to vary linearly with temperature. The limiting case, Ma=0, is the buoyancy driven convection problem typically referred to as the Rayleigh-Benard stability problem. The other limiting case, Ra=0, is the surface tension (gradient) driven flow problem referred to as the Marangoni-Benard problem. The equations and boundary conditions obtained from the linear analysis are solved numerically as a generalized eigenvalue problem. Neutral stability curves for different viscosity slopes have been generated for the Marangoni-Benard and Rayleigh-Benard problems. It is shown that the curves can be collapsed to a single curve by appropriately scaling the results for each of the limiting cases. The critical Marangoni number is determined as a function of the slope of the viscosity temperature variation, ε, for different values of the Rayleigh number. When the viscosity decreases linearly with temperature, the coupled buoyancy-surface tension problem, including the limiting cases of Ra=0 and Ma=0, is found to be more stable than the constant viscosity case.

14. SUBJECT TERMS

Marangoni-Benard convection; Variable viscosity; Temperature dependent viscosity; Rayleigh-Benard convection; Linear stability analysis

15. NUMBER OF PAGES

12

16. PRICE CODE

A03

17. SECURITY CLASSIFICATION OF REPORT	18. SECURITY CLASSIFICATION OF THIS PAGE	19. SECURITY CLASSIFICATION OF ABSTRACT	20. LIMITATION OF ABSTRACT
Unclassified	Unclassified	Unclassified	